



Reusable graphene oxide nanofibers for enhanced photocatalytic activity: a detailed mechanistic study

Shailendra Kumar Sharma¹, Shivali Sokhi², Chandrajit Balomajumder¹, and Soumitra Satapathi^{3,*}

¹Department of Chemical Engineering, Indian Institute of Technology Roorkee, Roorkee, Uttarakhand 247667, India

²Indian Institute of Science Education and Research, Mohali, Mohali, Punjab, India

³Department of Physics, Indian Institute of Technology Roorkee, Roorkee, Uttarakhand 247667, India

Received: 14 July 2016

Accepted: 10 January 2017

Published online:

23 January 2017

© Springer Science+Business Media New York 2017

ABSTRACT

Water pollution due to indiscriminate disposal of industrial dyes poses serious environmental hazards nationally and internationally. Some of the dyes are potentially carcinogenic and may induce mutagenicity and genotoxicity. Recently, graphene-based nanocomposite has attracted considerable interest for photocatalysis-based wastewater treatment. Here, we report the production of graphene-oxide-based hydrophobic PAN/GO nanofibers using electrospinning technique for photocatalytic degradation of Rhodamine 6G dye under natural sunlight illumination. The synthesized nanofibers were characterized using X-ray diffraction, EDX, field emission scanning electron microscopy and FTIR spectroscopy. Dye removal efficiency was investigated by monitoring UV–Vis absorption intensity over time. Structural change in dye was studied using FTIR analysis. Kinetics of dye degradation reaction was monitored through pseudo-first-order and pseudo-second-order kinetics model. Effects of nanofiber weight and initial dye concentration on the degradation efficiency were investigated in detail. Reusability and stability of these synthesized nanofibers in dye solution have been studied using scanning electron microscopy and FTIR spectroscopy. A comparative study for dye degradation was also performed using TiO₂-coated nanofibers under visible light and UV light illumination. These large-area reusable graphene oxide nanofibers provide a scalable and novel route for photocatalytic degradation of carcinogenic dyes from industrial water.

Introduction

Water pollution due to industrial coloring dyes is now an acute problem worldwide and in developing countries in particular [1]. It is estimated that 780

million people still lack the easy access to clean potable water. According to a recent report, it is estimated that around 37.7 million people are affected by water-borne diseases annually, 1.5 million children are estimated to die of diarrhea alone, and 73 million working days are lost due to water-borne

Address correspondence to E-mail: soumitrasatapathi@gmail.com

diseases each year (UNICEF and FAO Joint report). Some of the dyes are potentially carcinogenic and may induce mutagenicity and genotoxicity [2, 3]. Moreover, colored water reduces the penetration of light into the water thus altering the aquatic life. It also adds large quantity of chemicals in soil, thus affecting the eco-balance [4]. Various manufacturing industries such as textile, leather, pulp, paper, paint, food processing, cosmetics and plastics industries use dyes for coloring their products and produce almost 7×10^5 tones of dyes annually. These industries use huge amount of water, and abundant colored wastewater is discharged regularly to reservoirs [2, 5, 6]. Textile industry itself contributes to almost 20% of wastewater [7]. As a result, the removal of these toxic dyes from water is one of the major concerns of the scientific community today. It is proposed that 4% of the common disease burden can be relaxed by proper advancement of water supply system with sanitation and hygiene to maximize the health benefits [8].

Various physical, chemical and biological methods are reported in the literature for the treatment of colored wastewater. Some of the traditional methods for dye removal are adsorption on solid adsorbent [2, 4, 9] sedimentation, electrochemical coagulation and flocculation [10, 11]. In all these methods, pollutant is transferred from water to some another phase, thus generating secondary pollutant which further needs treatment. Moreover, there is problem of adsorbent regeneration in all these adsorption-based processes limiting their field application [12]. As potential alternative, engineered nanomaterial-based catalysis has gained significant interest recently due to large aspect ratio, tunable photo-physical properties, and quantum confinement effects of these nanomaterials [13]. Nanostructured materials such as nanoadsorbent, nanosize catalyst, nanomembrane, etc., give better selectivity and yield for the removal of pollutants from the wastewater [14]. 1D nanostructures are more effective catalyst than nanoparticles since nanocatalyst often leads to the formation of agglomerates, thus reducing the reactivity in solution [15]. Recently, graphene-based materials have attracted in fabricating the electronics devices and photocatalyst [16, 17]. Various methods are available for the synthesis of graphene such as chemical vapor deposition [18], epitaxial growth [19], micromechanical exfoliation [20] and reduction of

graphene oxide (GO) [21]. Among above, the reduction of GO to graphene is most economic method for bulk production. GO is usually prepared using Brodie, Staudenmaier and Hummers method, which involve the oxidation of graphite powder using acid followed by exfoliation of GO sheets. Graphene oxide has both sp^2 and sp^3 hybridized carbon atoms, and also additional chemical functionalization can be achieved in GO during synthesis process [15, 22]. The presence of sp^2 hybrid network in graphene-based materials makes them favorable for catalytic application [15, 23–25]. Graphene-based materials are extensively being used in photochemical or photocatalytic reactions for solar fuel generation [26], photocatalytic water splitting [27] and dye degradation [28–30]. Also the cost-effective production of nanofiber using electrospinning has advantage of large surface area and facile synthesis approach thus are commonly used in water remediation [31, 32].

Here, we demonstrated the production of graphene oxide (GO)/polyacrylonitrile (PAN) composite nanofibers by electrospinning method and their application for degradation of Rhodamine 6G (Rh6G) dye. Rh6G is xanthenes-based dye which is commonly used in different optoelectronics applications and as a coloring agent in various industries including cotton, silk, wool, fibers leather [33, 34]. It is a mutagen and hence highly toxic for cells, tissues and organisms. It is also proven to have carcinogenic and teratogenic effects [35, 36]. The Rh6G dye was completely photodegraded in the presence of GO/PAN nanofiber. Dye removal efficiency was investigated by monitoring UV–Vis absorption intensity over time. Structural change in dye was studied using FTIR analysis. Kinetics of dye degradation reaction was monitored through pseudo-first-order and pseudo-second-order kinetics model. Effects of nanofiber weight and initial dye concentration on the degradation efficiency were investigated in detail. Reusability and stability of these synthesized nanofibers in dye solution have been studied using scanning electron microscopy and FTIR spectroscopy. A comparative study for dye degradation was also performed using TiO_2 -coated nanofibers under visible light and UV light illumination. These large-area reusable graphene nanofibers provide a scalable and novel route for photocatalytic degradation of carcinogenic dyes from industrial water.

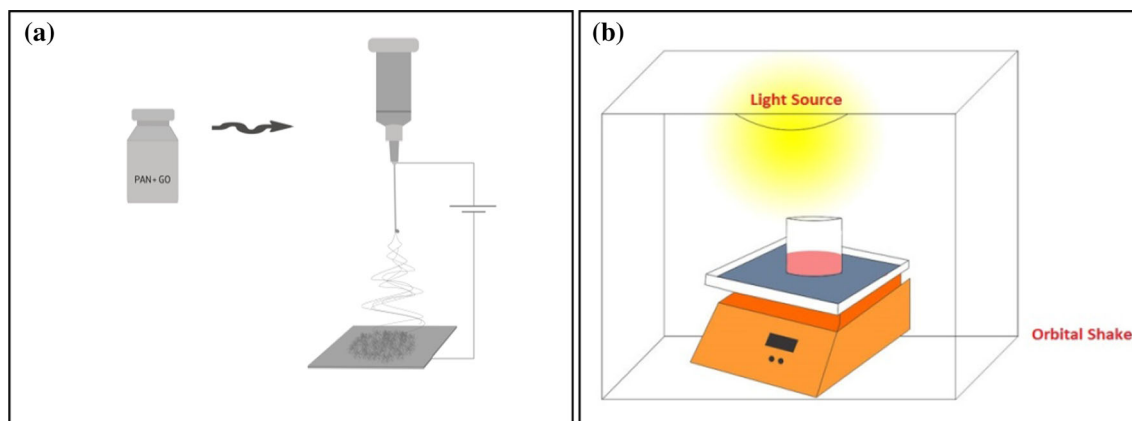


Figure 1 Schematic for **a** electrospinning setup, **b** photoreactor.

Materials and methods

Materials

Sodium nitrate (NaNO_3 , 99%), concentrated sulfuric acid (H_2SO_4 , 98%), potassium permanganate (KMnO_4 , 99%), hydrogen peroxide (H_2O_2 , 35%), Polyacrylonitrile (PAN), concentrated hydrochloric acid (36.5%), titanium tetra isopropoxide (TTIP, 99%) and Rhodamine 6G were purchased from Hi Media, Mumbai, India. Graphite powder was purchased from Bay Carbon Company, USA. All other solvents were purchased from Merck Ltd, Singapore.

Production of GO

Graphene oxide was synthesized using modified hummers method [37]. Briefly, 3 g of graphite powder was slowly added to concentrate $\text{H}_2\text{SO}_4 \cdot \text{NaNO}_3$ and solid KMnO_4 was slowly mixed under continuous stirring. The mixture was then kept in ice bath and stirred for another 2 h. Subsequently, the temperature was increased to 90 °C. After adding excess distilled water, the mixture was stirred using a magnetic stirrer for another 30 min. Finally, 30% H_2O_2 was added and the solution color changed to brilliant yellow.

Fabrication of the PAN/GO nanofibers

PAN/GO photocatalyst was synthesized using electrospinning technique. In typical procedure, an electrospinning solution composed of polyacrylonitrile (PAN) (1.75 g), GO (20 mg) and DMF (20 mL) was prepared. This solution was stirred for 24 h for uniform mixing. The electrospinning solution was taken

into a 5-ml syringe with a capillary tip whose inner diameter was 0.5 mm. A high potential of 13 kV was applied between the droplet at the needle of syringe and collector to generate high-intensity electric field as shown in Fig. 1a. A grounded electrode metal plate covered with 0.5-mm-thick aluminum foil was used as a collector. The collector was placed at a working distance of 15 cm. Flow rate of polymer solution was adjusted using syringe pump. The optimized flow rate was found to be 0.3 mL/h.

Synthesis of TiO_2

Titanium dioxide (TiO_2) sol-gel solution was synthesized using previously reported procedure [38], where 5 mL of titanium tetra isopropoxide (TTIP) and 0.8 mL of isopropyl alcohol (IPA) were slowly added to 30 mL of 0.1 M nitric acid solution under vigorous stirring. The solution was then refluxed at 80 °C for 12 h.

Synthesis of TiO_2 -loaded PAN/GO nanofibers

Synthesized PAN/GO nanofibers were coated with TiO_2 nanoparticles by dipping the nanofiber mat into TiO_2 sol-gel solution for 15 min for photocatalysis study. These fibers were then dried at 65 °C for 1 h in air.

Dye degradation study

Synthetic wastewater containing Rhodamine 6G was prepared by mixing different concentrations of Rhodamine 6G in water. PAN/GO nanofibers were added to this synthetic wastewater solution. The

solution was kept for continuous stirring for mixing and mobilizing the degraded dye from surface of nanofibers. The change in the concentration of dye

was studied using the change in peak absorbance of dye in UV–Vis spectra over time.

TiO₂-loaded PAN/GO nanofibers were used to study the photocatalytic degradation of Rhodamine 6G under visible light and UV light irradiation in a photocatalytic reactor. The experimental design of the photoreactor is shown in Fig. 1b. The photoreactor consists of an orbital shaker, a beaker with dye solution and a light source placed as shown. In this study, UV illumination and visible light bulb of 40 W were used as light sources. The beaker was placed onto orbital shaker to mobilize the degraded dye from surface.

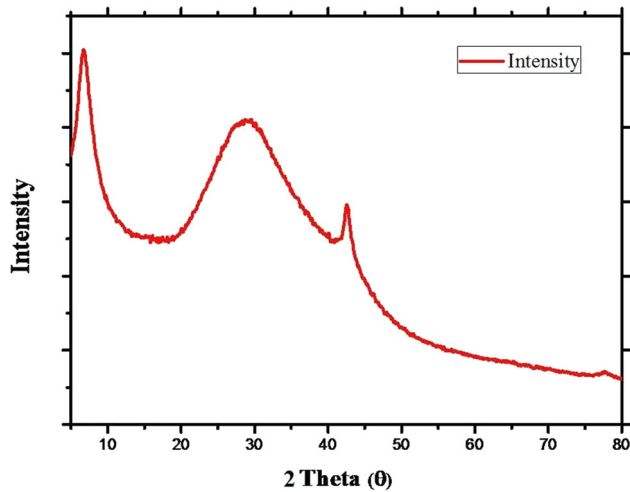
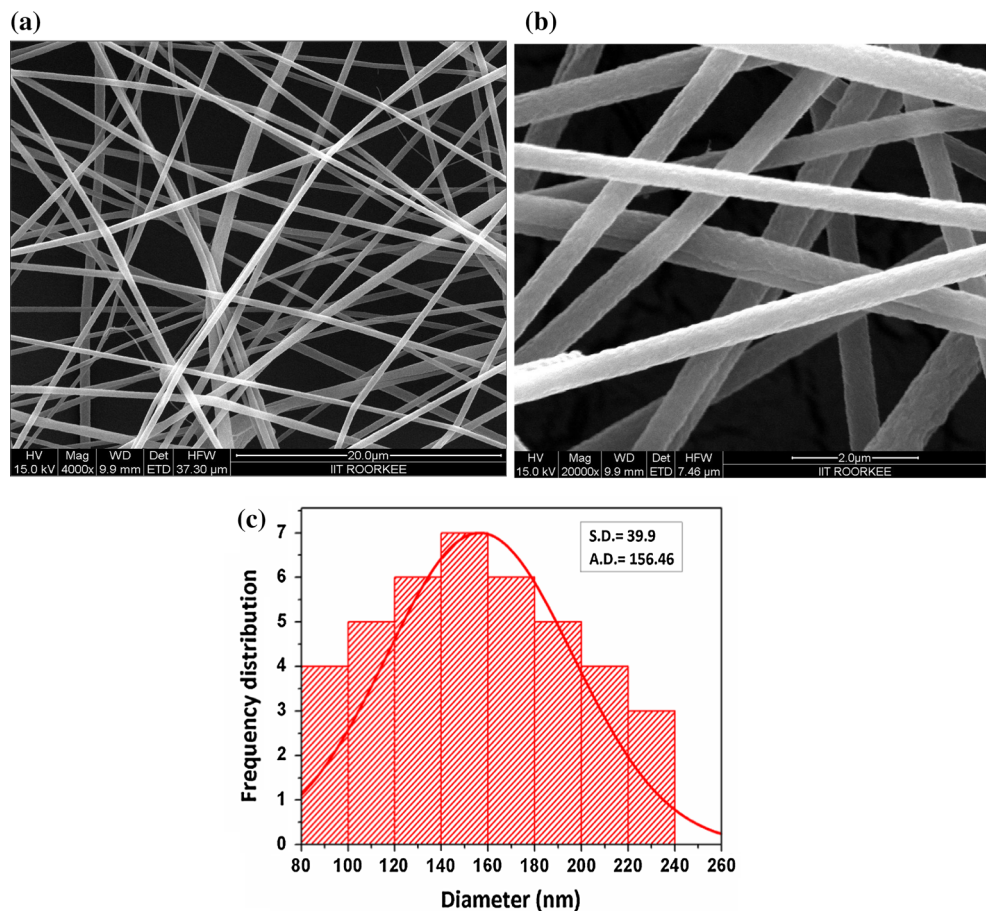


Figure 2 XRD pattern of graphene oxide (GO).

Characterization

The microstructure and surface morphology of the nanofibers samples were recorded by FESEM instrument (FEI Quanta 200 F, Netherland) operated at accelerating voltage of 15 kV. EDX was attached to FESEM. Surface morphology of nanofibers was also checked using scanning electron microscope (JEOL

Figure 3 a SEM image of nanofiber, b SEM image of nanofiber high resolution, c histogram for nanofiber diameter distribution.



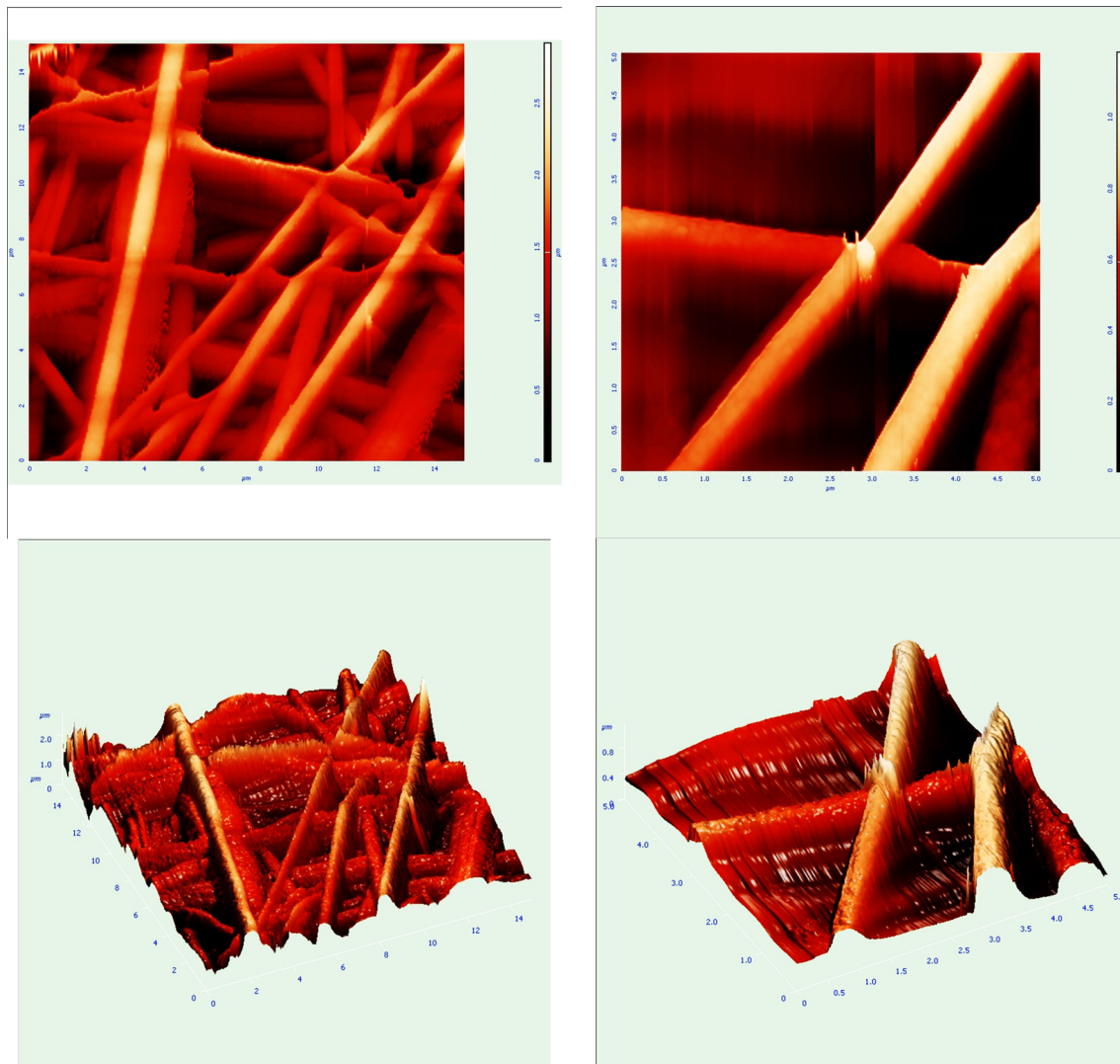


Figure 4 AFM image of nanofibers.

JEM2010) operated at 10 kV. NT-MDT NTEGRA was used to record AFM. UV–Vis spectrum for dye solution was recorded using Hitachi UV–Vis spectrophotometer. FTIR spectra of nanofibers and dye solution were obtained to understand the structure of PAN/GO nanofiber sample. FTIR was taken using a Thermo-Nicolet spectrometer using potassium bromide (KBr) pellets.

Results and discussion

Characterization of graphene oxide (GO)

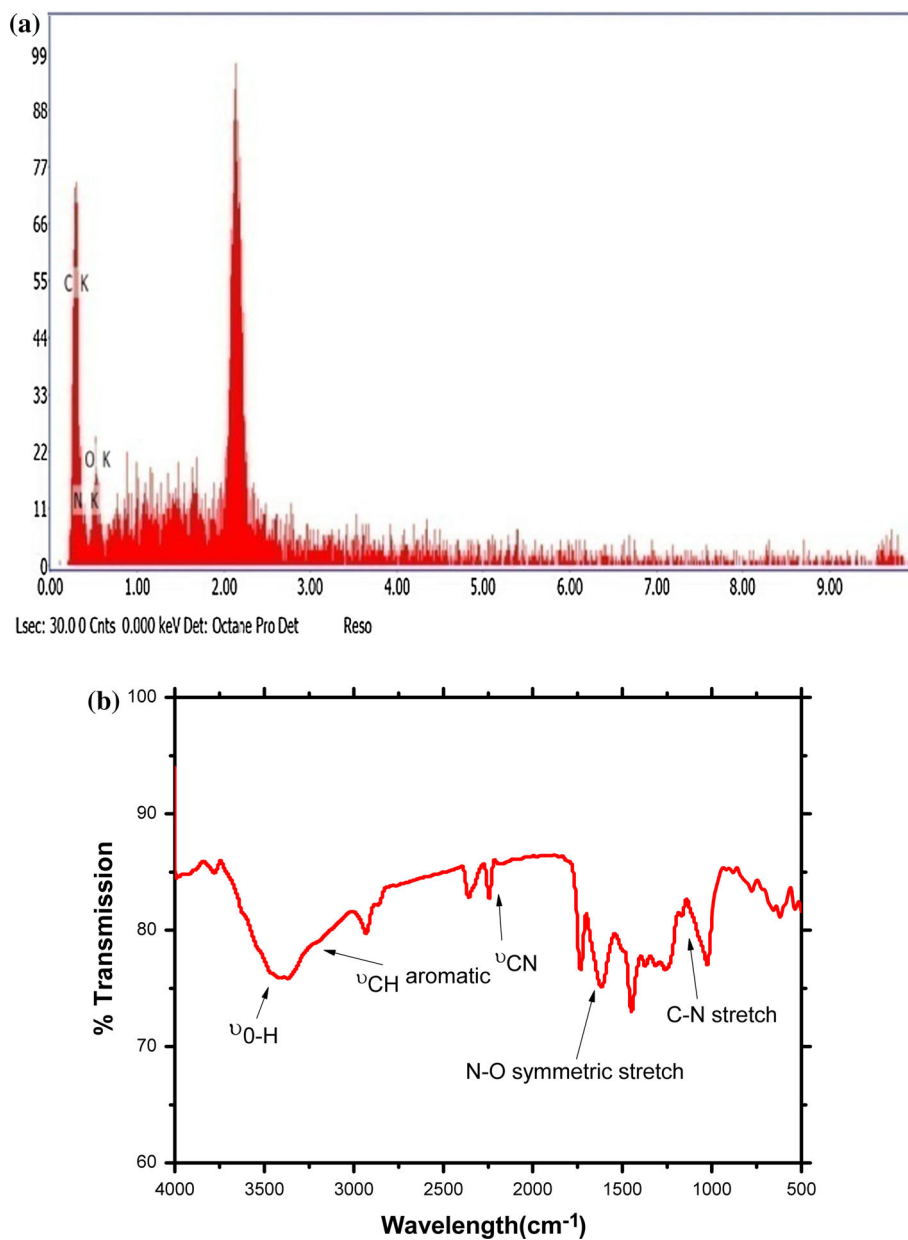
Figure 2 shows XRD pattern for synthesized GO; here, peak around 10° corresponds to characteristic

peak of GO which is from (002) plane reflection. Peak near 25° is from reduced graphene oxide (rGO) which comes due to incomplete oxidation of rGO, and peak at 43° comes from turbostratic band of disordered carbon materials which corresponds to (101) and (012) planes.

Characterization of PAN/GO composite nanofiber

Figure 3a shows the FESEM image of electrospun PAN/GO composite nanofibers with 9.26 wt% PAN and 0.1 wt% GO in DMF solution. The inset contains the high-magnification image. It shows that the obtained nanofibers are spread uniformly without aggregation. The average diameter of nanofibers was

Figure 5 **a** EDX spectra of nanofiber and **b** FTIR spectra of PAN/GO nanofiber.



estimated to be 156.46 ± 39.9 nm. Figure 3c shows the distribution of nanofiber diameter. The diameter of the nanofibers was found to be dependent on the electric field and flow rate. Since the nanofibers are a highly interconnected network resulting into a fibrous web, it provides a large surface area to dye solution. AFM image of the nanofibers is presented in Fig. 4, and image shows highly interconnected nanofibers overlapping each other. The energy-dispersive X-ray (EDX) analysis of electrospun nanofibers was carried out to find out the different elements present in the fiber mat. Figure 5a shows the obtained EDX spectra, which clearly implies that the

nanofibers are composed of carbon (C), nitrogen (N) and oxygen (O) atoms.

Figure 5b shows FTIR spectra of PAN/GO nanofibers before photodegradation experiment. The peak at 2224 cm^{-1} is from the $-\text{CN}$ groups of PAN, whereas peak at 3006 cm^{-1} represents C–H stretching vibration of the aromatic rings in GO. The peak observed at 1719 cm^{-1} corresponds to C=O stretching vibration. The peak at 1540 cm^{-1} can be attributed to N–O asymmetric stretching, whereas the peak at 1149 cm^{-1} is due to the C–N stretching in aromatic amines indicating the presence of aromatic amine groups in GO/PAN nanofibers. The broad band at

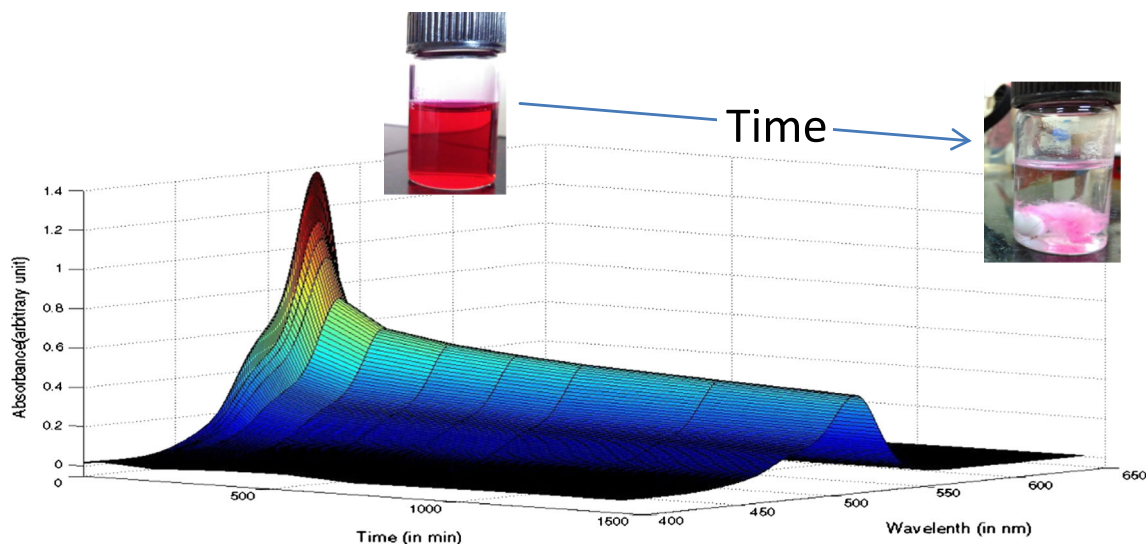


Figure 6 Degradation of dye over time.

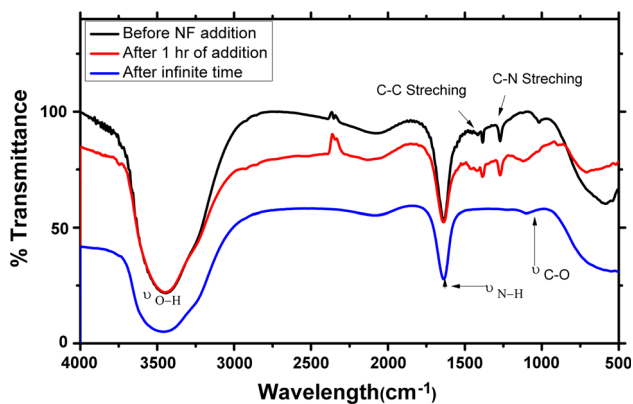


Figure 7 FTIR spectra of Rh6G dye nanofiber before and after the addition into nanofiber.

3755 cm^{-1} indicates that the nanofibers contain O–H group on their surface which interact with dye for efficient adsorption. GO FTIR peaks are consistent with previous report [39].

Photocatalytic degradation of dye

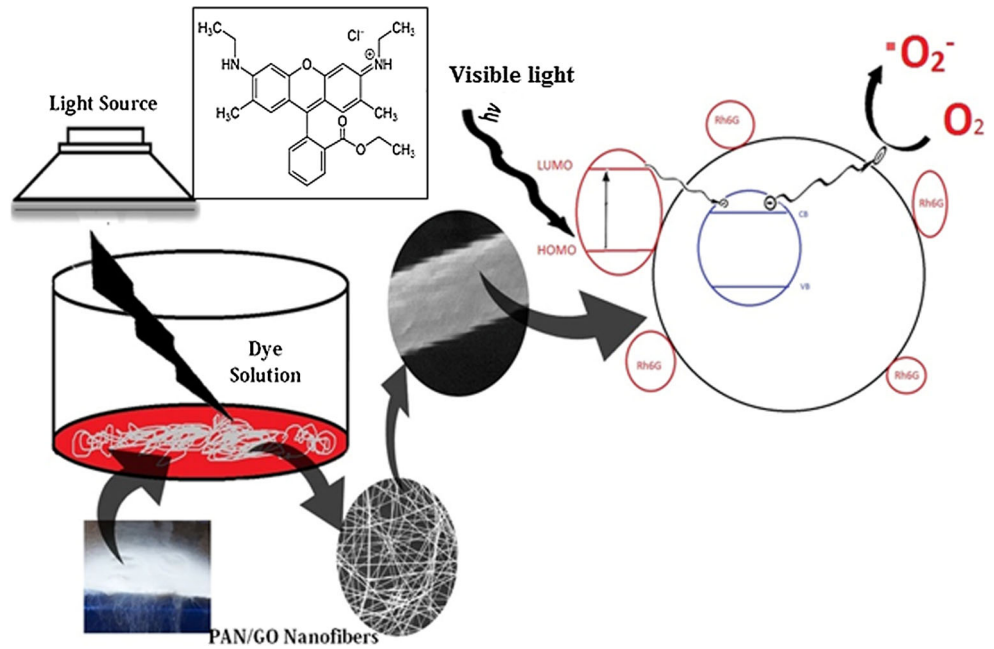
Photocatalytic degradation of dye was studied by dipping PAN/GO nanofibers into synthetic wastewater solution. The degradation efficiency was monitored by UV–Vis absorption spectroscopy. As shown in Fig. 6, the concentration of the Rh6G dye was degraded to 65% in 12 h under the natural sunlight with just 6 mg of nanofiber addition in 20 mL of dye solution. The color of the synthetic wastewater

also changes from dark red to almost transparent as shown in Fig. 6 making the photodegradation a colorimetric phenomenon.

Mechanism of dye degradation

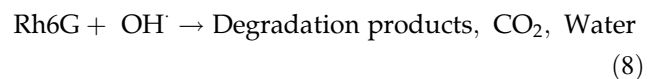
In order to understand the mechanism of the degradation process, FTIR spectra of Rh6G was taken before and after the nanofiber addition. Figure 7 presents FTIR spectra of Rh6G before PAN/GO nanofiber addition. As shown in Fig. 7, the peak at 1017 cm^{-1} corresponds to C–O stretching in ester group of Rh6G molecule, and the peak at 3457 cm^{-1} corresponds to the hydroxyl group (–OH) stretching, whereas the peak at 1639 cm^{-1} shows stretching vibration and scissor bending vibration of the amine groups. The small peaks at 1500, and 1471 cm^{-1} represent the vibration of aromatic ring (–C–C–), the band at 1268 cm^{-1} corresponds to the C–N stretching vibration, and the peak at 589 cm^{-1} corresponds to C–Cl stretching in Rh6G. The position and intensity of these bands get affected by nanofiber addition. Figure 7 shows the FTIR spectra of the Rh6G after the addition of PAN/GO nanofibers. The position and intensity of these bands changed after nanofiber addition. The FTIR spectra showed a blue shift in the 586 cm^{-1} band which corresponds to C–Cl stretching and the peak at 1017 cm^{-1} representing the C–O stretching has shifted to 1089 cm^{-1} with a marked decrease in transmittance. The peak corresponding to aromatic C–C stretch no longer exists in the solution with sufficiently long-time exposure to the

Figure 8 Mechanism of dye degradation in *inset* structure of Rhodamine 6G.



nanofibers. This can be attributed to the chemical interaction between Rh6G and PAN/GO nanofiber.

Based on the above observation, we propose a simple photocatalytic model for dye degradation (Fig. 8). At first, Rh6G molecules get adsorbed onto the nanofibers surface due to large aspect ratio of the nanofiber. This adsorption of dye can build up to multilayer. Figure S1 confirms the adsorption of Rhodamine 6G from wastewater onto the nanofibers. Later on, when light is absorbed by the photosensitizer dye molecule impregnated on the nanofiber surface, it excites the electron from HOMO energy level to LUMO energy level of Rh6G molecule. Photoexcited electron from Rh6G dye percolates through GO structure and transfers the electron rapidly to the oxygen molecule where it forms a highly reactive species O_2^- . This anion oxidizes H_2O to generate OOH^- anion. Two OOH^- anions then react to generate H_2O_2 . The H_2O_2 further dissociates to make $\cdot OH$ radical which is highly oxidizing agent and which degrades Rh6G to CO_2 , H_2O and other degradation products [40]. The following equations summarize the photocatalytic mechanism.



Effect of nanofiber weight

The effect of nanofiber amount on the dye degradation efficiency was studied using different weights of nanofibers, viz. 4, 6 and 8 mg with same concentration of dye. Figure 9 shows the decrease in dye absorbance over the time with different amounts of nanofibers. Rh6G degradation increases from 61.4% for 4 mg fiber to 90.6% for 8 mg over the period of 12 h as shown in Fig. 9c. This can be attributed to the availability of more catalytic sites due to increased exposed surface area of nanofibers leading to efficient photodegradation of dye.

Effect of dye concentration on degradation effectiveness

We also studied the photodegradation of Rh6G with different concentrations of dye. The dye degradation experiment was performed with three different concentrations of dye, namely 10^{-5} , 2×10^{-5} and 5×10^{-6} M, and the same amount of nanofiber (8 mg) was added. Figure 10 shows the degradation of dye with time, and it can be seen with the increase in dye concentration the percentage degradation

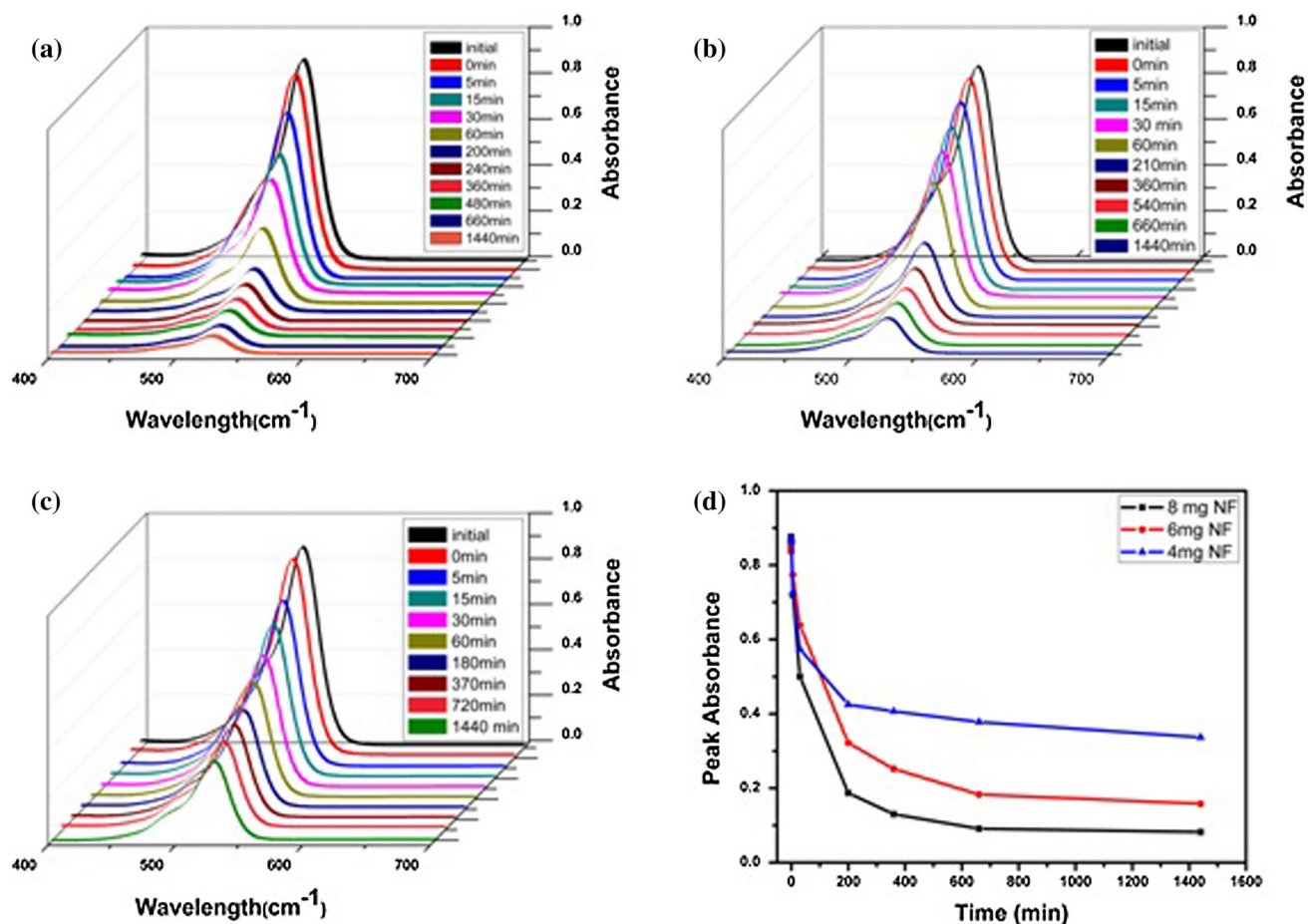


Figure 9 Photocatalytic degradation of Rhodamine 6G under natural sunlight **a** using 8 mg nanofiber, **b** using 6 mg nanofiber, **c** using 4 mg nanofibers.

decreases for same time period which is attributed to availability of more dye molecules for same surface area of nanofibers. Another reason for this is that once concentration of dye is increased, the dye will absorb the light and photon will never reach at photocatalyst surface [41].

Kinetic study

The quantity of dye adsorbed at a given time q_t (mg/g) and percentage dye removed were calculated according to the mathematical expressions below;

$$q_t = (C_i - C_t) \frac{V}{M} \quad (9)$$

$$\% \text{Removal} = \frac{(C_i - C_t)}{C_i} \times 100 \quad (10)$$

We calculated the first-order kinetics and second-order kinetics for the reaction. For the first order,

$$r = \frac{dC}{dt} = kKC = k_1C \quad (11)$$

$$\frac{dC}{dt} = k_1C \quad (12)$$

$$C = C_0 e^{-k_1 t} \text{ or } \ln\left(\frac{C_0}{C}\right) = k_1 t \quad (13)$$

Since we monitored degradation at 526 nm, the concentration in above mentioned equation can be written as

$$\ln\left(\frac{A_0}{A}\right) = k_1 t \quad (14)$$

Therefore, the curve between $\ln\left(\frac{A_0}{A}\right)$ and time (t) is a straight line with slope k_1 , where A_0 and A are absorbance at initial time and at some particular time of interest t .

Second-order kinetic model was also tried to fit for the data obtained from the experiment.

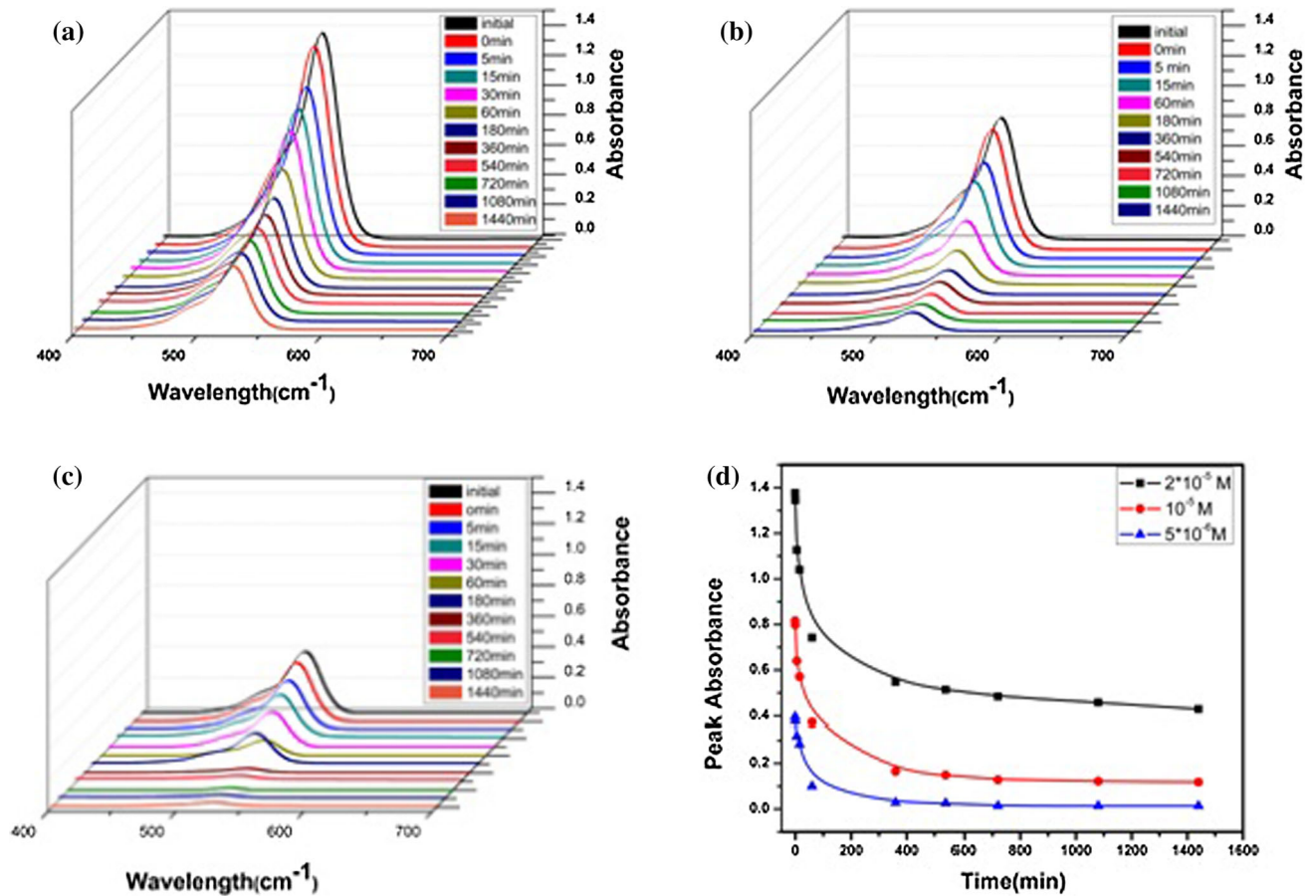


Figure 10 Photocatalytic degradation of Rhodamine 6G under natural sunlight **a** with 2×10^{-5} M Rh6G, **b** with 10^{-5} M Rh6G, **c** with 5×10^{-6} M Rh6G, **d** comparison in different concentrations.

$$r = \frac{dC}{dt} = k_2' C^2 \tag{15}$$

$$\frac{1}{C} = k_2' t + \frac{1}{C_0} \tag{16}$$

Replacing concentration by absorbance at characteristic wavelength

$$\frac{1}{A} = k_2 t + \frac{1}{A_0} \tag{17}$$

The resultant curve between $\frac{1}{A}$ and t was plotted.

Figure 11 describes the first- and second-order kinetics of degradation reaction. From Fig. 11, it can be inferred that the reaction does not clearly follow first-order or the second-order kinetics, and also it can be seen from the curve the degradation initially seems to follow the second-order kinetics and with the decrease in the dye concentration in the solution, the system tends to follow the first-order kinetics.

Reusability of PAN/GO nanofiber

Reusability is a key issue for a photocatalyst to be used for the industrial application. The used nanofibers were dried at 65 °C for 6 h and characterized with FTIR spectra to see the change in chemical structure of nanofibers. Figure 12c shows the FTIR analysis of the fibers after they were used for complete degradation. It can be seen from Fig. 12 that PAN/GO nanofibers represent same characteristic peaks before and after the addition of nanofibers to dye solution. It is clear from the spectra that chemical structure of the fibers remains the same after photocatalysis.

SEM images of fibers were also taken to see the effect on morphology of the nanofibers after using them for the removal of dye from the solution. FESEM images as shown in Fig. 12a depict negligible morphological change in the GO/PAN composite nanofibers after using them for degradation which

Figure 11 **a** Pseudo-first-order kinetics, **b** pseudo-second-order kinetics for 10^{-5} M Rh6G solution after the addition of 6 mg of PAN/GO nanofibers.

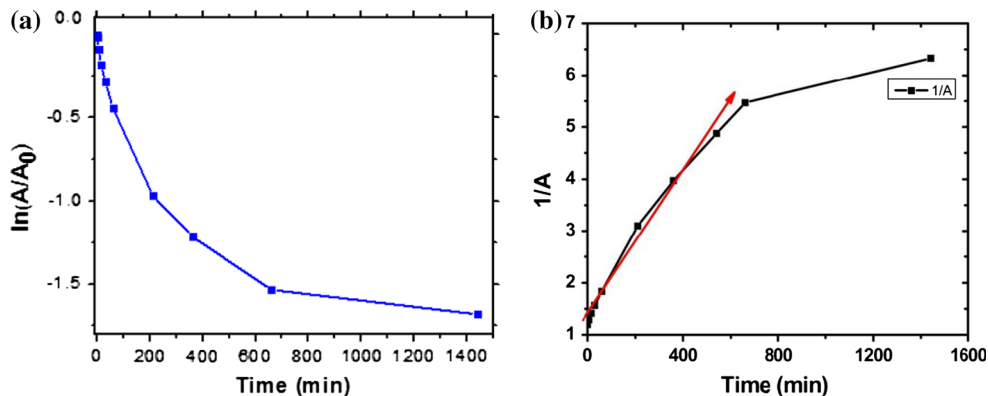
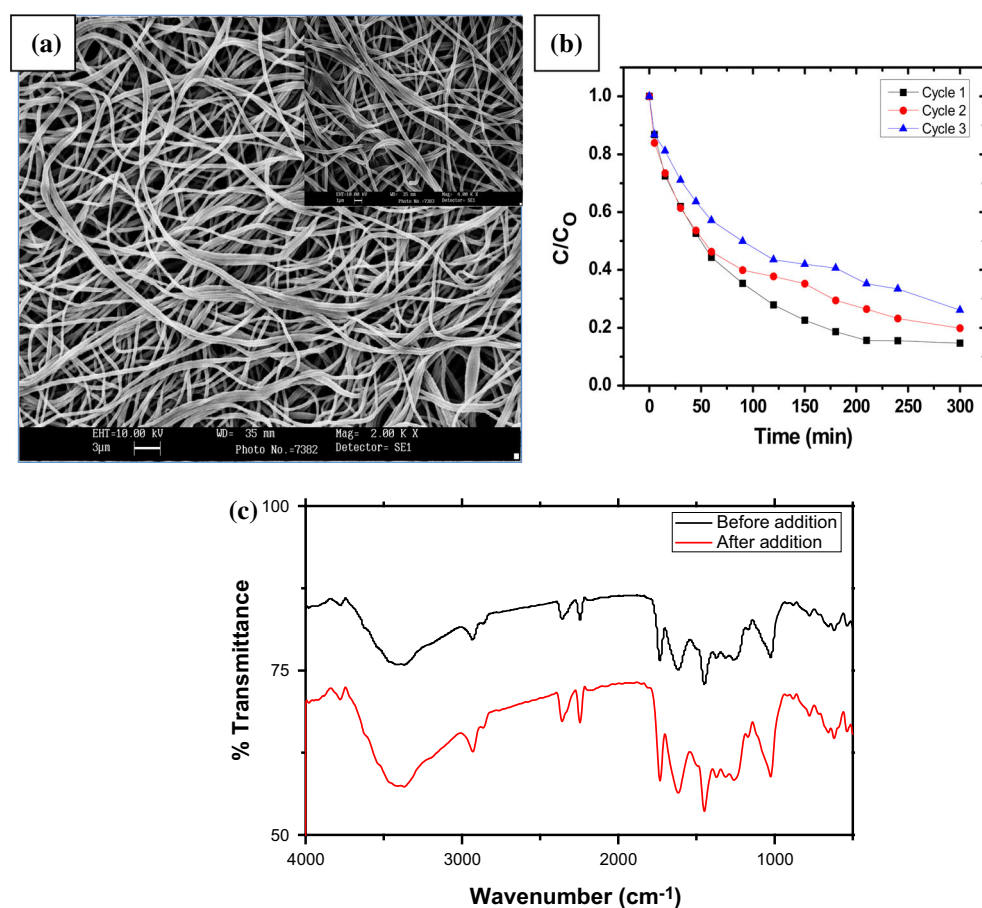


Figure 12 **a** SEM image of used PAN/GO nanofiber, **b** comparison of 2 cycles, **c** FTIR analysis of nanofiber before and after use.



proved the high stability of synthesized PAN/GO nanofibers.

Figure 12b shows the comparative study of photocatalysis after three successive cycles which shows very little performance change in degradation. It can be seen that after first cycle the degradation was about 85% and after three successive cycles the degradation does change from 84 to 74%. Therefore, these nanofibers can be reusable for dye degradation.

Photocatalytic degradation study using TiO_2 -loaded PAN/GO nanofibers

TiO_2 is widely studied semiconductor because of its good photocatalytic properties. We prepared composite TiO_2 -loaded PAN/GO nanocomposite by coating photocatalytic TiO_2 nanoparticles on the PAN/GO nanofibers to increase its photocatalytic activity as well as the effective surface area. These

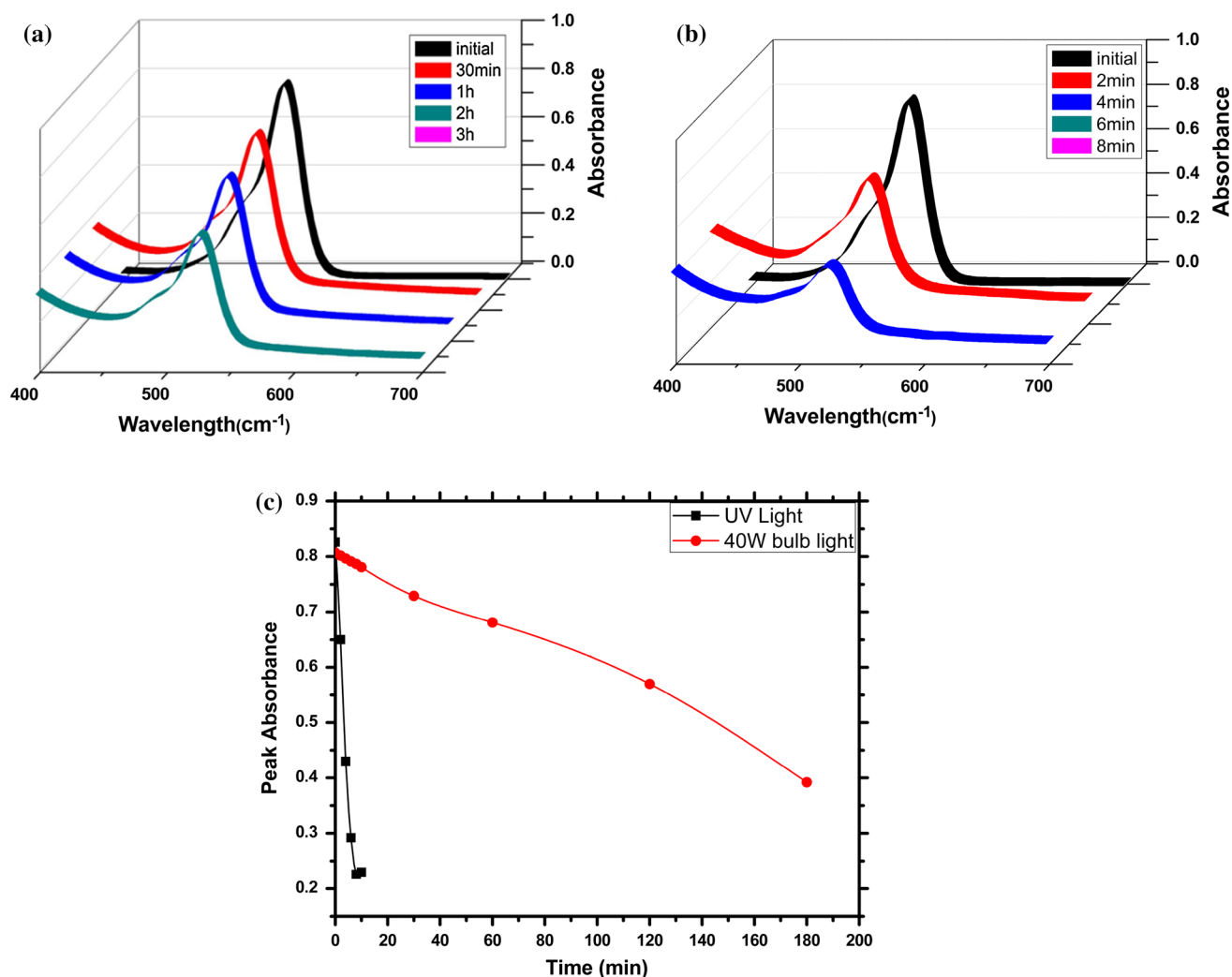


Figure 13 Degradation of dye using TiO₂-loaded PAN/GO nanofiber. **a** Under visible light illumination, **b** under UV light illumination, **c** comparison of dye degradation for UV and visible light.

nanofibers were used to study the degradation of Rh6G in visible light as well as in UV light. Figure 13 shows the degradation of Rh6G dye with time. The photocatalytic degradation of dye pollutant enhances with UV irradiation in comparison with fluorescent incandescent light.

The enhanced photocatalytic degradation with UV illumination could be attributed to the photoexcitation of TiO₂ along with the dye. TiO₂ onto nanofibers will absorb light (if $h\nu > E_g$) followed by the excitation of electron from VB to CB of TiO₂. Since GO has better electron and hole mobility than TiO₂, the excited electron is transferred easily to conduction band of graphene oxide which will readily transfer electron to O₂ making oxidizing species. Moreover, TiO₂ adsorbed onto the nanofiber will also funnel into the solution leaving trace amount of TiO₂

nanoparticles on the solution which will provide added photocatalytic properties; this can be seen in Fig. S2. The photoexcited electron from conduction band of TiO₂ (in solution) will lead to the formation of highly oxidizing species hydroxyl radical which will accelerate the degradation of dye [41, 42].

Conclusion

Here, we report the production of highly stable GO/PAN composite nanofibers using simple and facile electrospinning technique. FESEM confirms the formation of uniform nanofibers. FTIR and UV–Vis spectra of dye confirm that there is a strong interaction between nanofiber and Rhodamine 6G nanoparticles. The PAN/GO composite nanofibers

exhibited a good photocatalytic effect on Rhodamine 6G dyes degradation. Effect of various operational parameters onto the photocatalytic dye degradation was studied. The statistical analysis of experimental parameters such as initial dye concentration and amount of photocatalyst has significant effect on the removal of dye. It was observed that with the increase in the amount of photocatalyst, the process of degradation is faster. Similarly, the increased amount of dye will reduce the degradation rate. Furthermore, reusability and high stability are other advantages of these composite nanofibers. Effect of TiO₂ loading onto nanofiber suggests that with UV illumination, the dye degrade faster than visible light. The simple and elegant approach as proposed here provides a scalable and novel route for photocatalytic degradation of carcinogenic dyes from industrial water.

Acknowledgements

S.S like to acknowledge financial support from DST WTI (Grant No: DST/TM/WTI/2K2016/50(G)).

Electronic supplementary material: The online version of this article (doi:10.1007/s10853-017-0783-5) contains supplementary material, which is available to authorized users.

References

- [1] Kjellstrom T, Lodh M, McMichael T, Ranmuthugala G, Shrestha R, Kingsl S (2006) Air, water pollution: burden, strategies for control, ch. 43. In: Jamison DT, Breman JG, Measham AR et al (eds) Disease control priorities in developing countries, 2nd edn. World Bank, Washington
- [2] Yagub MT, Sen TK, Afroze S, Ang HM (2014) Dye and its removal from aqueous solution by adsorption: a review. *Adv Colloid Interface Sci* 209:172–184
- [3] Ratna P, Padhi BS (2012) Pollution due to synthetic dyes toxicity & carcinogenicity studies and remediation. *Int J Environ Sci* 3:940–955
- [4] Kaur S, Rani S, Mahajan RK (2013) Adsorption kinetics for the removal of hazardous dye congo red by biowaste materials as adsorbents. *Aust J Chem* 2013:12
- [5] Ajmal A, Majeed I, Malik RN, Idriss H, Nadeem MA (2014) Principles and mechanisms of photocatalytic dye degradation on TiO₂ based photocatalysts: a comparative overview. *RSC Adv* 4:37003–37026
- [6] Li Y, Xiao H, Chen M, Song Z, Zhao Y (2014) Absorbents based on maleic anhydride-modified cellulose fibers/diatomite for dye removal. *J Mater Sci* 49:6696–6704. doi:10.1007/s10853-014-8270-8
- [7] Kant R (2012) Textile dyeing industry an environmental hazard. *Nat Sci* 4:22–26
- [8] The world health organization, http://www.who.int/water_sanitation_health/facts_figures/en/. Accessed on April 2016
- [9] Garg VK, Gupta R, Yadav AB, Kumar R (2003) Dye removal from aqueous solution by adsorption on treated sawdust. *Bioresour Technol* 89:121–124
- [10] Gupta VK, Suhas S (2009) Application of low-cost adsorbents for dye removal—a review. *J Environ Manag* 90:2313–2342
- [11] Robinson T, McMullan G, Marchant R, Nigam P (2011) Remediation of dyes in textile effluent: a critical review on current treatment technologies with a proposed alternative. *Bioresour Technol* 77:247–255
- [12] Shukla A, Zhang YH, Dubey P, Margrave JL, Shukla SS (2002) The role of sawdust in the removal of unwanted materials from water. *J Hazard Mater* 95:137–152
- [13] Mittal A, Gupta VK, Malviya A, Mittal J (2008) Process development for the batch and bulk removal and recovery of a hazardous, water-soluble azo dye (Metanil Yellow) by adsorption over waste materials (Bottom Ash and De-Oiled Soya). *J Hazard Mater* 151:821–832
- [14] Akpan UG, Hameed BH (2009) Parameters affecting the photocatalytic degradation of dyes using TiO₂ based photocatalysts: a review. *J Hazard Mater* 170:520–529
- [15] Chen X, Zhang F, Wang Q, Han X, Li X, Liu J, Lin H, Qu F (2015) The synthesis of ZnO/SnO₂ porous nanofibers for dye adsorption and degradation. *Dalton Trans* 44:3034–3042
- [16] Zhang L, Diao S, Nie Y, Yan K, Liu N, Dai B, Xie Q, Reina A, Kong J, Liu Z (2011) Photocatalytic patterning and modification of graphene. *J Am Chem Soc* 133:2706–2713
- [17] Li H, Bubeck C (2013) Photoreduction processes of graphene oxide and related applications. *Macromol Res* 21:290–297
- [18] Sutter PW, Flege JI, Sutter EA (2008) Epitaxial graphene on ruthenium. *Nat Nanotechnol* 7:406–411
- [19] Berger C, Song Z, Li X, Wu X, Brown N, Naud N, Mayou D, Li T, Hass J, Marchenkov AN, Conrad EW, First PN, de Heer WA (2006) Electronic confinement and coherence in patterned epitaxial graphene. *Science* 312:1191–1196
- [20] Novoselov KS, Geim AK, Morozov SV, Jiang D, Zhang Y, Dubonos SV, Grigorieva IV, Firsov AA (2004) Electric field effect in atomically thin carbon films. *Science* 306:666–669

- [21] Stankovich S, Dikin DA, Piner RD, Kohlhaas KA, Kleinhammes A, Jia Y, Wu Y, Nguyen ST, Ruoff RS (2007) Synthesis of graphene-based nanosheets via chemical reduction of exfoliated graphite oxide. *Carbon* 45:1558–1565
- [22] Georgakilas V, Otyepka M, Bourlinos AB, Chandra V, Kim N, Kemp KC, Hobza P, Zboril R, Kim KS (2012) Functionalization of graphene: covalent and non-covalent approaches, derivatives and applications. *Chem Rev* 112:6156–6214
- [23] Wang H, Maiyalagan T, Wang X (2012) Review on recent progress in nitrogen-doped graphene: synthesis, characterization, and its potential applications. *Acs Catal* 2:781–794
- [24] Xiao S, Shen M, Guo R, Wang S, Shi X (2009) Immobilization of zerovalent iron nanoparticles into electrospun polymer nanofibers: synthesis, characterization, and potential environmental applications. *J Phy Chem C* 113:18062–18068
- [25] Singaravel GP, Hashaikeh R (2016) Fabrication of electrospun LTL zeolite fibers and their application for dye removal. *J Mater Sci* 51:1133–1141. doi:10.1007/s10853-015-9444-8
- [26] Xiang Q, Cheng B, Yu J (2015) Graphene based photocatalysts for solar fuel generation. *Angew Chem Int Ed Engl* 54:11350–11366
- [27] Xiang Q, Yu J (2013) Graphene-based photocatalysts for hydrogen generation. *J Phys Chem Lett* 4:753–759
- [28] Yang MQ, Xu YJ (2013) Selective photoredox using graphene-based composite photocatalysts. *Phys Chem Chem Phys* 15:19102–19118
- [29] Fu D, Zhang L, Xie R, Xu H, Zhong Y, Sui X, Mao Z (2016) Fabrication of novel rGO/Bi₂O₃/TiO₂ heterojunction for enhanced visible-light photocatalytic activity. *J Photochem Photobiol A* 329:18–25
- [30] Roso M, Lorenzetti A, Boaretti C, Hrelja D, Modesti M (2015) Graphene/TiO₂ based photo-catalysts on nanostructured membranes as a potential active filter media for methanol gas-phase degradation. *Appl Catal B* 176:225–232
- [31] Garg B, Bisht T, Ling YC (2014) Graphene-based nanomaterials as heterogeneous acid catalysts: a comprehensive perspective. *Molecules* 19:14582–14614
- [32] Malwal D, Gopinath P (2016) Fabrication and applications of ceramic nanofibers in water remediation: a review. *Crit Rev Environ Sci Technol* 46:500–534
- [33] Im JS, Kim MI, Lee YS (2008) Preparation of PAN-based electrospun nanofiber webs containing TiO₂ for photocatalytic degradation. *Mater Lett* 62:3652–3655
- [34] Kubin RF, Fletcher AN (1983) Fluorescence quantum yields of some rhodamine dyes. *J Lumin* 27:455–462
- [35] Selwyn JE, Steinfeld JI (1972) Aggregation of equilibria of xanthene dyes. *J Phys Chem* 76:762–774
- [36] Choyke PL, Alford R, Simpson HM, Duberman J, Craig Hill G, Ogawa M, Regino C, Kobayashi H (2009) Toxicity of organic fluorophores used in molecular imaging: literature review. *Mol Imaging* 8:341–354
- [37] Shahriary L, Athawale AA (2014) Graphene oxide synthesized by using modified hummers approach. *Int J Renew Energy Environ Eng* 2:58–63
- [38] Yan F, Huh P, Li L, Wang Y, Samuelson LA, Kumar J (2009) Photovoltaic performance enhancement in dye-sensitized solar cells with periodic surface relief structures. *J Macromol Sci* 46:1213–1216
- [39] Wang Q, Du Y, Feng Q, Huang F, Lu K, Liu J, Wei Q (2013) Nanostructures and surface nanomechanical properties of polyacrylonitrile/graphene oxide composite nanofibers by electrospinning. *J Appl Polym Sci* 128:1152–1157
- [40] Malwal D, Gopinath P (2015) Fabrication and characterization of poly (ethylene oxide) templated nickel oxide nanofibers for dye degradation. *Environ Sci Nano* 2:78–85
- [41] Daneshvar N, Salari D, Khataee AR (2003) Photocatalytic degradation of azo dye acid red 14 in water: investigation of the effect of operational parameter. *J Photochem Photobiol A* 157:111–116
- [42] Asiri AM, Al-Amoudi MS, Al-Talhi TA, Al-Talhi AD (2011) Photodegradation of Rhodamine 6G and phenol red by nanosized TiO₂ under solar irradiation. *J Saudi Chem Soc* 15:121–128